J Seismol (2006) 10:247–257
DOI 10.1007/s10950-006-9010-6

ORIGINAL ARTICLE

M_L determination for local and regional events using a sparse network in Southwestern Germany

Stefan Stange

Received: 23 July 2004 / Accepted: 10 January 2006

Abstract A method for the determination of consistent local magnitude M_L values (Richter scale, or M_{WA}) for earthquakes with epicentral distances ranging from 10 km through 1000 km is demonstrated. The raw data consists of nearly 1300 amplitude readings from a network of six digital seismographs in Baden–Württemberg (Southwestern Germany) during 26 months starting in 1995, later extended by another 1000 amplitude readings until 1999. Relying on most of the basics introduced by C.F. Richter a three-parameter attenuation curve (distance correction, magnitude-distance relation) for Baden–Württemberg and adjacent areas is presented. Station corrections are evaluated and the attenuation curve is calibrated with respect to other agencies for distances greater than 650 km. Reasonable parametrisations are discussed and meaningful error bars are attributed. Finally, a seventh station is incorporated by means of its station correction alone, without needing to update the attenuation curve.

Keywords Local magnitude M_L · Attenuation curve · Station correction · Bootstrap error bars · European earthquakes

S. Stange (✉)
Regierungspräsidium Freiburg,
Referat Landeserdbebendienst Baden-Württemberg;
Landesamt für Geologie
Albertstrasse 5
79104 Freiburg i. Breisgau, Germany
e-mail: stefan.stange@rpf.bwl.de

Introduction

Even in the age of digital seismographs and computer-aided data processing the importance of the magnitude concept still persists. Originally, Richter (1935, 1958) used solely the maximum amplitude of horizontal seismograms from Wood–Anderson (WA) seismometers to compute his magnitude (M_L, local magnitude or M_{WA}) with the aid of a distance correction, which is not very smooth compared to more recent proposals (Fig. 1).

For an absolute calibration of his magnitude scale, Richter (1935) used a pivotal point (called the *Richter hinge* in this study) at a distance of 100 km where 1mm WA-amplitude was defined as magnitude 3.0. Hutton and Boore (1987) proposed an accordant magnitude-three hinge for 10 mm WA-amplitude at a distance of 17 km.

While there exist better concepts for the quantification of the earthquake source (e.g. Ben-Zion, 2001), the magnitude as a relative scale is widely in use albeit its use is not beyond doubt (Hough, 2001 and replies in Seismological Research Letters, Vol. 71). It is popular, not only, among seismologists but also for public information, and a great number of variations, extensions and improvements to the original idea of Richter have been proposed (e.g. Jennings and Kanamori, 1983; Kim, 1998 for Eastern North America; Ferdinand, 1998; Langston et al., 1998 for East Africa).

The intention of this paper is not merely to add to this variety and to propose a magnitude formula especially

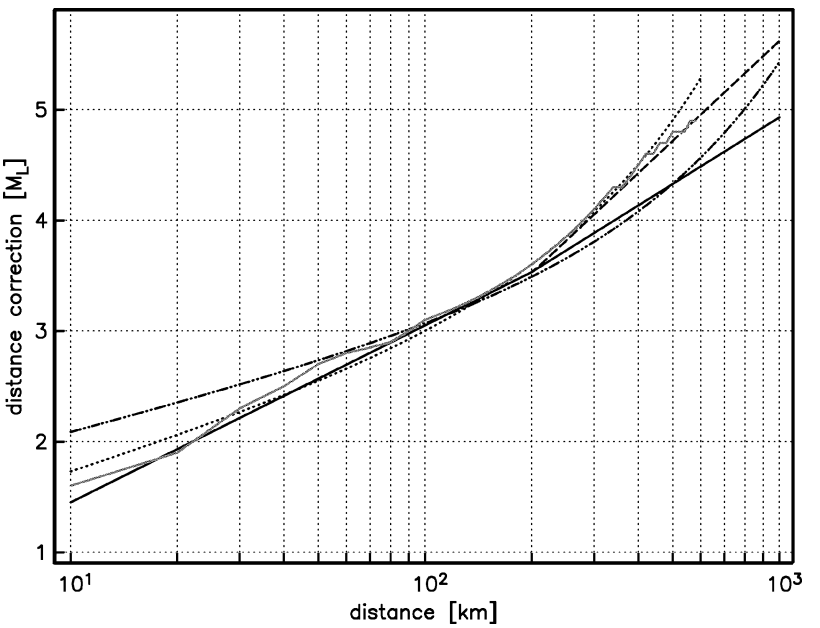

Fig. 1 Distance correction curves for M_L from various authors: LED from 1996 through 1997 (solid line); parameterisation of Richter (1958) in use from 1983 through 1996 (dashed line); Bakun and Joyner (1984) (dotted line); SZGRF at 1 Hz (K. Klinge, pers. comm.) (dash–dotted line); Richter original (1958) (gray line)

suited for Baden–Württemberg without changing the maximum–amplitude concept of Richter. But moreover, an improved use of existing concepts is detailed and a single magnitude calculation for a small network in a big area (such as Europe) is suggested. It is shown that the local magnitude M_L can be meaningfully extended up to a distance of 1000 km and that for these great distances the tuning to agencies nearer to the epicenter is important for sparse and small–aperture networks. Error considerations are introduced and the essential importance of station corrections is elucidated.

The reason for continuing with the maximum–amplitude concept and not adopting moment magnitude (Kanamori, 1977) is outlined below. First of all, consistency and continuity within the catalogue of an agency is deemed very important. Following Kanamori (1983), the differences between moment magnitude and local magnitude are restricted to a constant offset and therefore are negligible compared to other uncertainties (see below for the discussion of error bars) up to a magnitude of about six. Hence, there is no need to switch to moment magnitude since the historical catalogue for earthquakes in Germany (Leydecker, 1986) does not list any events with a magnitude of more than six and a half and only a few events that may exceed six. Furthermore, for small earthquakes recorded with solely short period instruments the computation of the moment magnitude by means of a moment tensor inversion is not feasible.

Instrumental earthquake observation in Baden–Württemberg (Fig. 2) has a history of over a century (Schick and Wielandt, 1994). In Württemberg, the eastern part of the state area mapped in Fig. 2, the earthquake survey was maintained by the University of Stuttgart, and up to 1993 the original Richter formula for magnitude determination was in use. In Baden (western part, University of Karlsruhe) modern earthquake observation started in 1973. From 1983 to 1993 a simple parameterization of the Richter distance correction (Fig. 1) was utilized. In 1993 the Earthquake Survey (LED) of the State Bureau of Geology, Natural Resources and Mining (NEIC code is LEDBW) succeeded its two predecessors as the defining agency. Temporarily, the magnitude determination was adopted from Karlsruhe and the distance correction was improved in 1996 for distances beyond 200 km (Fig. 1). The official and actual magnitude formula (in application since 1997) is developed in this paper, observing as much continuity and integration with the European seismological community as possible.

The necessity of an improved magnitude formula for Baden–Württemberg is evidently illustrated by a display of the data from station KIZ (Kirchzarten, see Table 1): Fig. 3 displays the magnitude readings at KIZ computed with the magnitude scale in use until 1997

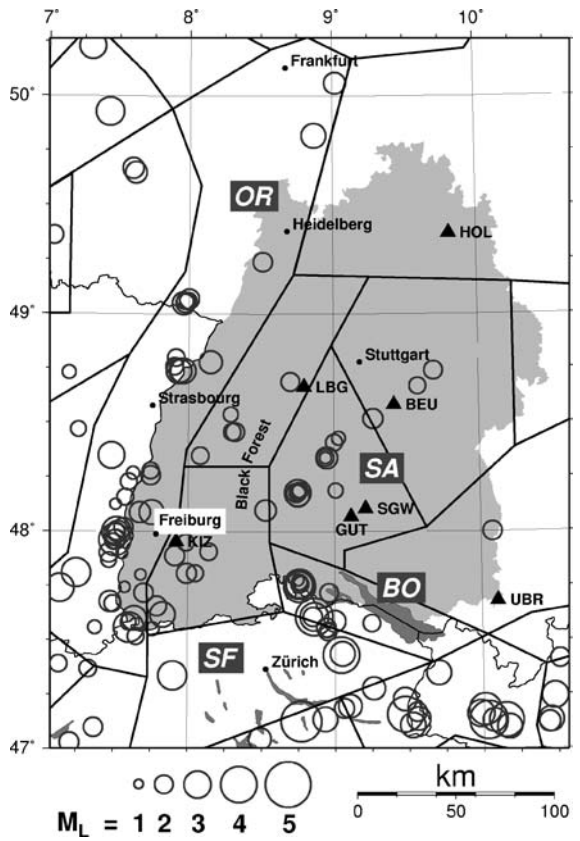

Fig. 2 Baden-Württemberg (light shaded area), the south–western state of Germany, bordering France and Switzerland. Black triangles denote the station network, open circles are some epicenters used in this study. Outlined areas with white-on-black labels are selected seismo–geographical regions after Leydecker and Aichele (1998): OR (Upper Rhine Graben), SF (Eastern Swiss Alpine Foreland), BO (Lake of Constance), SA (Swabian Jura)

(Fig. 1). The normalization with respect to the event magnitude denoted by the horizontal line at zero offset exhibits two clear features: the first is the general offset that can be dedicated to the lack of a station correction (constant for all distances). The second is a distance dependent trend that might be due to the use of a non–optimal attenuation curve.

Stations and data

Seven stations (Fig. 2) were selected from the 30-station monitoring network operated in Southwestern Germany by the LED (Henger and Leydecker, 2000; Brüstle and Stange, 2002). These stations are equipped with Lennartz LE3D-1 Hz seismometers and Mars88 20-bit data loggers recording at a 16 ms sampling interval. The transfer function is proportional to ground velocity and is flat from 1 Hz to 25 Hz. The seven seismograph systems are identical to each other, well calibrated, and provide vertical as well as horizontal components. The latter are routinely used for M_L determination.

Station site underground conditions are fairly diverse as listed in Table 1. The seismometers are located in basements of water storage basins, in abandoned mines, and in underground bunkers (vaults).

The maximum aperture of the 7-station-network measures slightly over 200 km in the SW-NE direction; mean station distance is in the order of 80 km (Fig. 2).

Data contribution of individual stations is moderately inhomogeneous as listed in Table 1, because the installation of the network in Baden–Württemberg was in progress during the recording period. In general, station GUT did not participate at first, since it was opened only in October 1997 to replace SGW, which had to be closed down.

For the first data set 293 events (of which at least 99 percent are earthquakes) in the period from January 1995 to March 1997 were evaluated, resulting in a total of 1300 good–quality amplitude readings. The epicenters are distributed over central and southern Europe showing a lopsided distribution towards southern directions. Epicentral distances range from 10 km (Upper Rhine Graben, Black Forest, Swabian Jura, cf. Fig. 2) up to 1000 km (Vienna Depression, Balkan countries, Central/Southern Italy, Pyrenees).

Data processing

The basic principles of amplitude measurement from three–component stations are as follows. Firstly, the seismograms of a station should show at least one phase (P or S) which can be unequivocally picked. Further, the horizontal traces must not be truncated before the largest amplitudes (S or Lg) and must also not be clipped. If strong transient signals unrelated to the earthquake in question are present the corresponding traces are omitted.

After band pass filtering from 0.5 Hz to 12 Hz and integration both whole traces are equalized and amplified to simulate a Wood–Anderson instrument with an eigenperiod of $T = 0.8$ s, a damping of $h = 0.8$, and

Table 1 Stations participating in the study with number of data, resulting station correction, stratigraphy/lithology, and site description

Station	No. of data	Station correct.	Stratigraphy	Lithology	Site
KIZ Kirchzarten	255	+0.28	Palaeozoic	Gneiss (diatexite)	Mine
HOL Hollenbach	140	−0.14	Pleistocene/Unterkeuper	Clay over dolomite	Storage basin
UBR Überruh	209	−0.08	Upper Fresh water–Molasse	Marl/siltstone	Storage basin
LBG Lerchenberg	223	+0.07	Künzelsauer Schichten	Bioclastic limestone	Vault
BEU Beuren	197	−0.08	Wedelsandstein	Sandy limestone	Vault
SGW Sigmaringen	247	−0.05	Liegende Bankkalke	Bedded limestone	Storage basin
GUT Gutenstein	147	+0.25	Oberer Massenkalk	Massive limestone	Storage basin

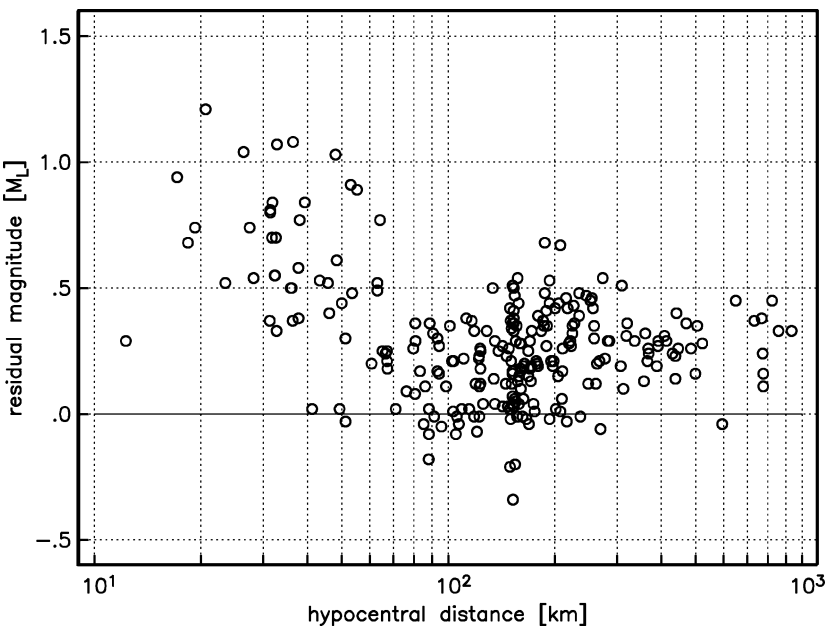

Fig. 3 Station KIZ: residual magnitudes (event magnitude minus station magnitude) for 255 events with the pre-1997 distance correction and without station correction

an amplification of $S = 2800$. These are the *classical* values although Urhammer et al. (1996) determined the *correct* values for real Wood–Anderson seismometers which were never in use in Baden–Württemberg. The peak maximum amplitude from both horizontal components of a record is measured separately and the two values are averaged. At last the logarithm of the mean is calculated.

To compute magnitude values for each station (this station magnitude is abbreviated M_{ST}) from the amplitude readings one needs the distance to the hypocenter which comes with the localisation process. The event magnitude (M_{L} which is assigned to the event in the catalogue) is then derived by computing the median of the station magnitudes. The median is less sensitive to outliers than the mean, and it is used in the L_1–norm context (Shearer, 1997).

Methodology for the distance correction

The amplitude of a traveling seismic wave is affected by geometrical spreading as well as intrinsic attenuation and scattering. In a homogeneous medium the geometrical spreading of body waves is proportional to r^{-1} where r is the hypocentral distance. In an arbitrary medium this can be generalized to a power law of the form r^{-a}. Published empirical values for the exponent a range from 0.8 through 2 (a comprehensive compilation is found in Bormann and Bergman, 2002). Further sophisticated descriptions of the geometrical

spreading account for structural effects and therefore introduce a distance dependence (e.g. Douglas et al., 2004, or see below in this publication).

The attenuation (including intrinsic damping and scattering) is described by $e^{-\gamma r}$ where $\gamma = 0$ for a medium without any attenuation. Common values of γ are around 0.002 (Bormann and Bergman, 2002) but they depend strongly on wave type and medium. Easier to handle, in some cases, is the parameter b which is defined by $b = \gamma \log e \approx \gamma/2.3$.

With these considerations in mind and following for instance Bakun and Joyner (1984) the basic equation for the magnitude at station ST reads:

$$M_{\mathrm{ST}} = \log\ A + a\ \log r + br + c + d_{\mathrm{ST}} \tag{1}$$

where A is the Wood–Anderson amplitude in mm, and the distance r is measured in km. a and b are the spreading and attenuation parameters introduced above while the third parameter c defines an absolute level and can be determined by the Richter hinge at 100 km. The station correction d_{ST} is discussed in a later section.

While the parameters a, b, and c can be derived from the data using a standard least–squares scheme, the event magnitude M_{L} is calculated as the median of the station magnitudes M_{ST} (see above). Hence, the overall procedure to derive M_{L} from the data is slightly non–linear. Linearization can be achieved by using differential parameters instead of the original ones. This again requires start values for M_{L} since the linearized inversion can only calculate differences to these (i.e. $\Delta M = M_{\mathrm{ST}} - M_{\mathrm{L}}$). Additionally, iteration may lead to an incremental improvement and sufficient convergence.

Implementation of the iterative procedure exhibited that the resulting attenuation curve was independent of the start values except for the greatest epicentral distances. Hence, reasonable start values for these longest distances had to be introduced. They were taken from other agencies or networks [e.g.: SED (Zürich), INGV (Roma) and LDG (Paris)] which could consider the event in question to be of "local" character. This improved the result considerably in two ways: first, the inversion for the correction curve was stabilized and second, a good degree of consistency with other agencies in Europe was obtained for the longest distance range without biasing the *local* range.

Unfortunately, there was only rather sparse information about the magnitude calibration of the other agencies. Therefore, the large uncertainty resulted in low confidence for this data. Nevertheless, the far end of the correction curve was reduced by more than one magnitude compared to other estimates (Fig. 1).

For earthquakes nearer home start magnitudes were simply taken from the previous calculations with the Richter parametrization of the distance correction curve (see above).

Other means of constraining the attenuation curve are described in a later section.

Results

With the data and inversion methodology introduced in the previous sections the magnitude–distance relation for earthquakes observed in Baden–Württemberg reads:

$$M_{\mathrm{L}} = \log\ A + (1.11 \pm 0.1)\ \log r + (0.95 \pm 0.2) \times 10^{-3}\, r + (0.69 \pm 0.05). \tag{2}$$

In the following this magnitude scale is called BWAC (abbreviation of *Baden–Württemberg attenuation curve*) and it is plotted in Fig. 4. The variance reduction compared to the LED–Richter parametrisation (Fig. 1) is 14 percent.

Since this result was obtained through least–squares inversion, numerical error bars (standard deviations) can be attributed. With almost 1300 data samples and only three parameters small errors are to be expected for Gaussian distributed data.

A problem will occur if the data distribution is not normal. In this case standard deviations of a least–squares inversion may underestimate *realistic* error bars significantly. For instance, Stange and Friederich (1993) reported an underestimation factor of up to 10. As a workaround Efron and Gong (1983) proposed the so called bootstrapping technique. The basics are as follows: secondary data sets are created by randomly drawing from the original data pool with "put–back". Hence, a new set may contain multiple entries of a data point while other samples may not be present at all. The same inversion as described above is now computed for, say, 1000 new data sets. The scatter of the solutions gives an indication of Gaussian error bars.

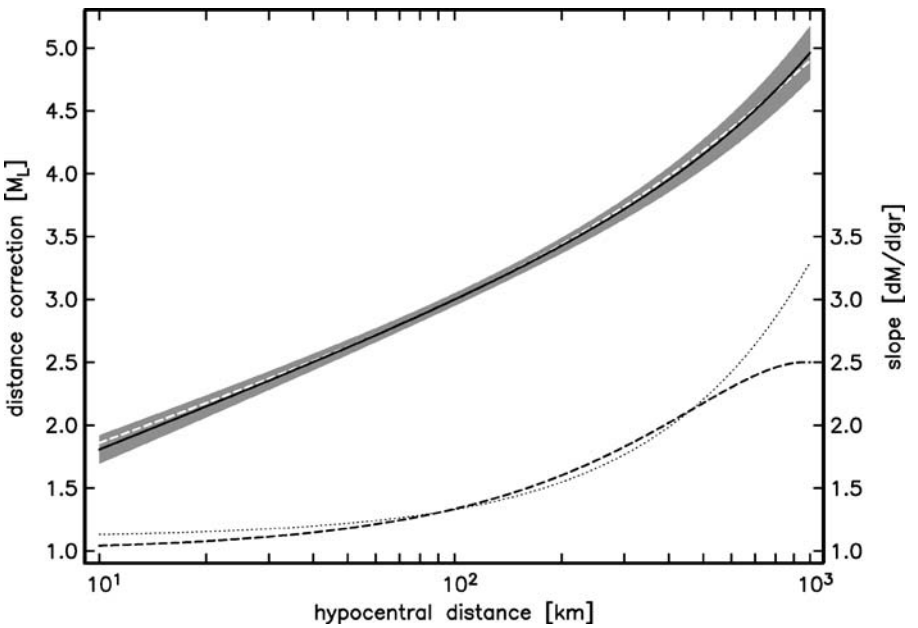

Fig. 4 Graphical representation of Equation (2): BWAC distance correction (black line) with 68 percent confidence level (shaded area) from the bootstrap procedure. The white dashed line represents Equation (6) with its local slope $dM/\mathrm{d}\log r$ (dashed black). Dotted: local slope of BWAC

Furthermore, features like bimodal distributions would show up in the collection of solutions.

It should be mentioned that the bootstrap is only used to calculate the error bars and not for computing the best value of a parameter itself, since this can only be accomplished with the original data set. On the other hand, a consistency check showed that the mean of the bootstrap solutions sufficiently resembled the original least–squares result. The bootstrap data sets were choosen to exactly match the number of entries of the original. Up to 1500 inversions were then performed and stabilty of the results was ensured.

Since the bootstrap–computed standard deviations are considered the most meaningful in this study they are denoted in Equation (2). They exceeded the least–squares standard deviations by a factor of up to 10.

The bootstrap–errors of the three parameters of the distance curve (Equation (2)) can be combined with the Gauss' law of error propagation to obtain a single one–standard deviation or 68–percent confidence interval as sketched in Fig. 4 (shaded area). Note the influence of the Richter hinge: at a distance of 100 km the error range reduces to that of the constant term, i.e. the standard error of the mean of the station corrections. At short distances the error of the spreading term dominantes while at long distances the largest error contribution arises from the attenuation term.

For most events the final standard deviation for the network computed magnitude M_L lies around ± 0.2.

A competing solution: Distance dependent parameters

Up to now, it was argued that for Baden–Württemberg one simple 3-parameter curve could sufficiently describe the magnitude–distance correction for 10 km to 1000 km. Though, this kind of parametrisation is deemed inadequate for instance by Bragato and Tento (2005) for NE–Italy. One suggested reason for the success in Baden–Württemberg is the smooth development of seismogram characteristics with distance. However, there still exists a transition from the body–wave regime to a surface–wave regime.

On one hand, this concerns geometrical spreading: very near the source body waves are supposed to behave like spherical waves, that is their amplitudes are proportional to r^{-1}. At long distances the magnitude determining Lg waves undergo surface-wave-like spreading, which was given by Kvamme et al. (1995) for Scandinavia to be proportional to $r^{-0.71}$.

On the other hand, the transition affects the attenuation due to anelasticity and scattering which was assumed to be modelled by $\gamma = 2\text{–}3 \times 10^{-3}$ for body waves, and was determined to $\gamma = 1.8\text{–}2 \times 10^{-3}$ for western European Lg waves (Nicolas et al., 1982).

Finally, in the same paper the entire amplitude attenuation coefficient for Lg waves in western Europe is shown to be roughly 2.5×10^{-3} which translates into a local slope of $d\mathrm{M}/d \log r = 2.5$.

Omitting the station correction in Equation (1) the distance correction can be rewritten in a more general form:

$$M = \log\ A + a(r) \log r + 10^{-3} b(r) r + c \tag{3}$$

where both $a(r)$ and $b(r)$ are distance–dependent functions of the form:

$$a(r) = a_0 - 10^{-3} a_1 r \quad \text{and} \quad b(r) = b_0 - 10^{-3} b_1 r. \tag{4}$$

Rearranging Equations (3) and (4) into:

$$M = \log\ A + a_0\ \log\ r + 10^{-3} b_0 r + c - (a_1\ \log\ r + 10^{-3} b_1 r) \times 10^{-3} r \tag{5}$$

facilitates another interpretation of the new attenuation curve description. The first terms (featuring a_0, b_0, and c) are easily recognised as the original 3-parameter curve. The later part might be read as a correction term in form of another attenuation curve weighted with distance.

As described in the previous section the sparse network suffers a certain lack of resolution. Hence, it is recommended to reduce the degrees of freedom by introducing boundary conditions. Here, besides the Richter hinge ($M|_{100} = 3$), two further restrictions were used: the local slope of the correction curve was fixed to a value of 2.5 at a distance of 1000 km: $d\mathrm{M}/d \log r|_{1000} = 2.5$. And, the geometrical spreading at short distances should be around 1, hence, it was set: $a_0 = 1$.

Least–squares inversion of the data set for the remaining 2 parameters resulted in:

$$M_\mathrm{L} = \log A + (1 - 0.29 \times 10^{-3} r) \log r + (2.2 - 0.28 \times 10^{-3} r) \times 10^{-3} r + 0.84. \tag{6}$$

This representation is rather descriptive: the effective spreading parameter starts at a distance of 1 km for instance, with a value very near unity ($a \approx 1$) and then decreases to a value of $a = 0.71$ at 1000 km, matching nicely the properties of body and surface waves as sketched above. Similarly, the attenuation parameter b varies from 2.2 ($r = 1$ km) to 1.92 ($r = 1000$ km)(a factor of 10^{-3} is absorbed in the distance term). As intended, the local slope rises from $d\mathrm{M}/d \log r|_1 = 1$ to $d\mathrm{M}/d \log r|_{1000} = 2.5$ (Fig. 4), contrary to BWAC where $d\mathrm{M}/d \log r|_{1000}$ exceeds 3.3. Furthermore, Fig. 4 also shows that the absolute difference between BWAC and the curve given by Equation (6) exceeds 0.07 magnitudes at no point.

Unfortunately, while Equation (6) might provide a reasonable physical interpretation it is far from being a unique solution. Other parameter combinations are possible or even entirely differing mathematical descriptions. Some authors (e.g. Urhammer et al., 1996) proposed the use of spline functions to smooth a distance correction curve which was originally obtained in distance sections. Of course, more degrees of freedom might provide a further variance reduction.

Variance reduction of Equation (6) is 19 percent, compared to 14 percent of BWAC (Equation (2)). But, is there a significant difference? Comparing two distributions with their variances can be conducted by means of a so-called F–test (Press et al., 1986). The F-test calculates the probability of the null-hypothesis that two distributions do not differ. F-testing the variances of Equation (2) and Equation (6) offers a probability near 1, which means that for the presented data set no significant improvements compared to BWAC could be achieved.

Even so, if one considers distances around and beyond 1000 km, only the constant–slope extrapolation of the curve from Equation (6) would yield a reasonable correction for Lg magnitudes.

Station corrections

Station corrections compensate for that part of the site effect which is invariant with azimuth. The station magnitude mainly depends on station underground conditions, e.g. shear wave velocity V_S or attenuation Q_S averaged over a specific depth range. Urhammer et al. (1996) gave a relationship between near-surface rigidity μ and station correction. Unfortunately, this cannot

be applied here, since the absolute values they computed were dependent on the particular distance correction chosen.

To get a qualitative idea of individual station corrections one can inspect the surface lithology of the station sites as compiled in Table 1. On a relative scale the end members would be marked by stations HOL and KIZ, respectively. Station HOL is situated on a thin layer of pleistocene clay overlying mesozoic dolomite. It is therefore expected to show some kind of amplitude amplification, and thus greater than average station magnitudes. On the other hand, station KIZ is located 50 meters underground in an abandoned mine of the Schauinsland ore district, in solid bedrock (gneiss). Station magnitudes for KIZ are presumed to be systematically lower than the event magnitude. The data shown in Fig. 3 (station KIZ) actually supports the tendency anticipated from the lithological site conditions.

In principle, the computation of station corrections using Equation (1) is straightforward although not advisable due to the following considerations: first, the mean of the station corrections is indistinguishable from the constant c of the distance correction. Second, the non–uniform data distribution with distance might introduce systematic biases. To avoid these drawbacks station corrections were computed using a modified data set: only events with amplitude readings at all six stations were used, resulting in 93 events with 558 readings (out of 1300 for the entire data set). Furthermore, the data were assigned to distance bins of a width of 20 km to achieve equal contributions from all distances.

The overall inversion now followed an iterative dual step approach, alternating between the computation of distance correction and station corrections, respectively. A similar approach was proposed by Hutton and Boore (1987). Final convergence was reached after three iterations, which is considerably faster than the 20–40 iterations reported by Langston et al. (1998). The results are listed in Table 1. Variance reduction is now 43 percent compared to the previously achieved 14 percent, meaning that two thirds of the overall variance reduction are due to station corrections.

The distance correction turned out to be rather stable during iteration, hence justifying the dual step approach in retrospect. This invariance of the distance correction is also important for the incorporation of new stations into an existing network.

How does an extension of the recording network affect the magnitude computation? An opportunity to research this question arose at the end of 1997 when station SGW had to be closed due to extensive construction work at the water storage basin nearby. The equipment was moved about 8 km to the west to the new location GUT (Fig. 2). The geological setting was nearly identical (Table 1), hence, about the same station correction (-0.05 for SGW) could be expected. After a recording period of more than a year 222 events had been collected, out of which 143 showed more than 5 decent amplitude readings. Station GUT contributed 147 readings, 84 of which are in the latter data set.

With the inversion scheme described above the distance correction (Equation (2)) remained almost unchanged while the station correction for GUT computed to $+0.25$, severly contradicting the expectations.

To address this puzzling issue station SGW was reinstalled for three months in 1999. Earthquakes recorded simultaneously at GUT and SGW at once revealed strong amplitude differences. Therefore, surface lithology obviously does not suffice to explain this site effect. On the other hand, SGW is situated a mere few hundred meters from the east edge of the Lauchert Graben, a prominent tectonic feature of the south–central Swabian Jura. This structure might affect SGW amplitudes, but, a detailed examination has to be relegated to future research.

Source region and propagation path effects

Figure 5 displays residual magnitudes for station KIZ, recomputed with BWAC and station correction. Comparison with Fig. 3 illustrates the improvement and corresponds to the reasonable variance reduction (43 percent). Although, at distances shorter than 100km the absolute values of the residuals seem to be larger than average. Of course, the scatter of the data at short distances should increase since source radiation effects are more pronounced here. But, this cannot explain the pattern visible in Fig. 6. Evidently, the residual magnitudes depend on the seismotectonic region of most of the events shown: high values at distances below 65 km correspond to events from the Upper Rhine Graben (cf. Fig. 2) while low values at distances greater than 60 km are located in the regions of Lake Constance and Swiss Eastern Alpine Foreland. These two clusters separate clearly in azimuth and distance, and therefore the cause of the differences is mainly the propagation path to

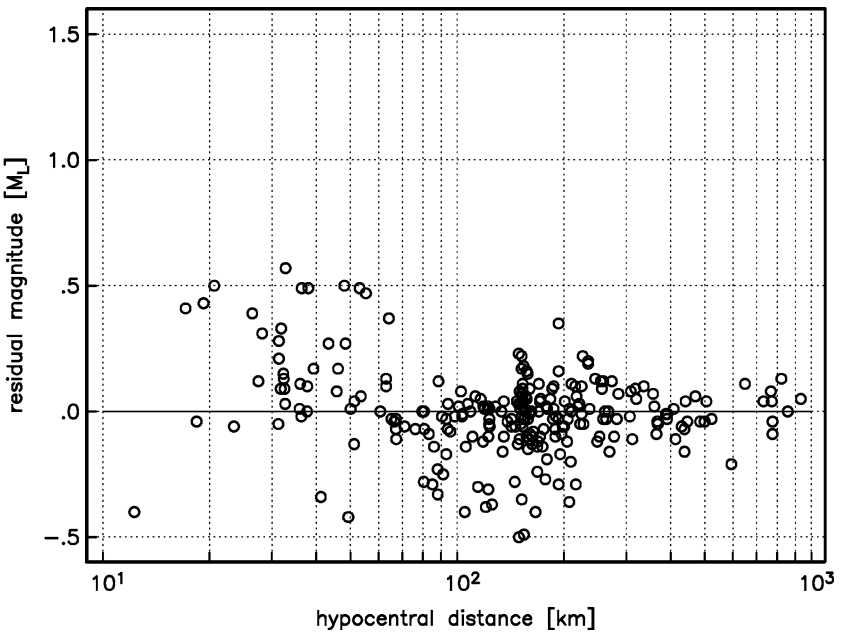

Fig. 5 Same as Fig. 3, now computed with new distance correction BWAC and with station correction for KIZ

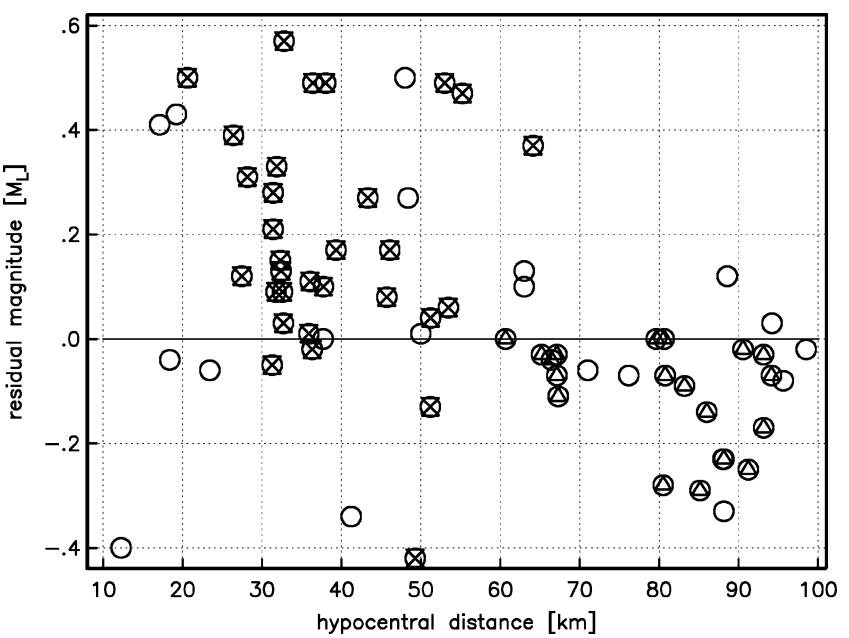

Fig. 6 Same as Fig. 5 for distances below 100 km. Grey circles: all events. Events from the seismo–geographic regions (see Fig. 2) OR (hourglasses); BO and SF (triangles) are enhanced

station KIZ. The residual magnitudes of other stations (not shown) did not exhibit a matchable pattern, therefore, a mere distance dependence of this effect could be excluded.

With the concept of constant station corrections, effects such as those shown in Fig. 6 cannot be accounted for. However, the interpretation of this phenomenon remains conjectural and would have to be examined by a detailed study of source and propagation effects with an extended data base.

Conclusion

In this study it was demonstrated that with a medium–size (aperture around 200 km) and sparse (6 to 7 stations) seismograph network reasonable magnitudes

M_L can be calculated for hypocentral distances from 10 km through 1000 km. Though, some precautions have to be observed, which are outlined below.

Firstly, distance correction curves developed for a different region (e.g. California) might produce misleading results, or might be applicable only over a limited distance range. Therefore, a customised distance correction should be computed. Furthermore, calibration of the long–distance end of a new attenuation curve with respect to neighbouring agencies is recommended. This is especially important within the European surrounding where there exist quite a few independent agencies but no unified magnitude specification.

Second, station corrections are essential for a consistent determination of a network magnitude by averaging station magnitudes. The introduction of station corrections accounted for two thirds of the variance reduction achieved in this study.

Finally, the incorporation of new seismometer stations can be done through their station correction alone, without changing the attenuation curve. This seems to be self–evident, but, for the described sparse and medium–size network it had to be verified, and it could be useful for networks under construction.

Assigning meaningful error bars to a magnitude helps asses the scatter between agencies, although, it is not helpful for public information.

The presented procedure for computing local magnitudes was included in the New Manual for Observatory Practice (Bormann and Bergman, 2002).

Acknowledgements First of all I wish to thank Dr. W. Brüstle for his support, encouragement, and advice for this publication and on many other matters. Comments by John Douglas, Jürgen Strehlau, and an anonymous reviewer greatly improved the manuscript. Mainly, John Douglas helped converting my style into decent English. Further, the support of the staff of the LED is thankfully acknowledged. Dr. M. Franz is thanked for his help with the geological information. Figure 2 was drawn using GMT (Wessel and Smith, 1991). The other figures were plotted with PLOTXY by Robert Parker and Loren Shure. Some of the computer programs were based on recipies from Press et al. (1986).

References

Bakun WH, Joyner WB (1984) The M_L scale in central California. Bull Seis Soc Am 74:1827–1843

Ben–Zion Y (2001) On quantification of the earthquake source. SRL 72:151–152

Bormann P, Bergman E (eds) (2002) The new manual of observatory practice. GeoForschungsZentrum Potsdam, Germany

Bragato PL, Tento A (2005) Local magnitudes in northeastern Italy. Bull Seis Soc Am 95.2:579–591

Brüstle W, Stange S (2002) Earthquakes in Baden–Württemberg, 2000; Bulletin of the Earthquake Survey of the State Bureau for Geology, Natural Resources and Mining Baden–Württemberg, Freiburg

Douglas J, Suhadolc P, Costa G (2004) On the incorporation of the effect of crustal structure into empirical strong ground motion estimation. Bull Earthquake Engineering 2(1):75–99

Efron B, Gong G (1983) A leisurely look at the bootstrap, the jackknife and cross–validation. The American Statistician 37:36–48

Ferdinand RW (1998) Average attenuation of 0.7–5.0 Hz *L*g waves and magnitude scale determination for the region bounding the western branch of the East African Rift. Geophys J Int 134:818–830

Gasperini P (2002) Local magnitude revaluation for recent Italian earthquakes (1981–1986). J Seis 6.(4):503–524

Henger M, Leydecker G (eds) (2000) Erdbeben in Deutschland 1994, Bundesanstalt für Geowissenschaften und Rohstoffe, Hannover, p 47

Hough S (2000) On the scientific value of "Unscientific" data. SRL 71:483–485

Hutton LK, Boore DM (1987) The M_L scale in southern California. Bull Seis Soc Am 77:2074–2094

Jennings PC, Kanamori H (1983) Effect of distance on local magnitudes found from strong–motion records. Bull Seis Soc Am 73:265–280

Kanamori H (1977) The energy release in great earthquakes. J Geophys Res 82:2981–2987

Kanamori H (1983) Magnitude scale and quantification of earthquakes. Tectonophysics 93:185–199

Kim W-Y (1998) The M_L scale in Eastern North America. Bull Seis Soc Am 88:935–951

Kvamme LB, Hansen RA, Bungum H (1995) Seismic–source and wave–propagation effects of *L*g waves in Scandinavia. Geophys J Int 120:525–536

Langston CA, Brazier R, Nyblade AA, Owens TJ (1998) Local magnitude and seismicity rate for Tanzania, East Africa. Bull Seis Soc Am 88:712–721

Leydecker G (1986) Erdbebenkatalog für die Bundesrepublik Deutschland mit Randgebieten für die Jahre 1000–1981, in: Geologisches Jahrbuch, E36, 3-83, Bundesanstalt für Geowissenschaften und Rohstoffe, Hannover.

Leydecker G, Aichele H (1998) Seismogeographical regionalisation of Germany: the prime example for third–level regionalisation. in: Geologisches Jahrbuch, E55, 85–98, Bundesanstalt für Geowissenschaften und Rohstoffe, Hannover.

Nicolas M, Massinon B, Mechler P, Bouchon M (1982) Attenuation of regional phases in western Europe. Bull Seis Soc Am 72:2089–2106

Press WH, Flannery BP, Teukolsky SA, Vetterling WT (1986) Numerical Recipes. Cambridge University Press, New York, p 993

Richter CF (1935) An instrumental earthquake magnitude scale. Bull Seis Soc Am 25:1–31

Richter CF (1958) Elementary Seismology. W. H. Freeman and Co., San Francisco, pp 578

Schick R, Wielandt E (1994) Zur Geschichte der instrumentellen Erdbebenbeobachtung und Erdbebenforschung in Württemberg und Hohenzollern. Jh Ges Naturkde Württemberg 149:75–98

Shearer PM (1997) Improving local earthquake locations using the L1 norm and waveform cross correlation: application to the Whittier Narrows, California, aftershock sequence. J Geoph Res 102:8269–8283

Stange S, Friederich W (1993) Surface wave dispersion and upper mantle structure beneath Southern Germany from joint inversion of network recorded teleseismic events. Geoph Res Lett 20:2375–2378

Uhrhammer RA, Loper SJ, Romanowicz B (1996) Determination of local magnitude using BDSN broadband records. Bull Seis Soc Am 86:1314–1330

Wessel P, Smith WHF (1991) Free software helps map and display data. EOS Trans Amer Geophys U 72(441):445–446